International Journal of GEOMATE
(Geotechnique, Construction Materials and Environment)
ISSN: 2186-2982 (P), 2186-2990 (O), Japan

Vol. 31, Issue 144, August, 2026, PP. 30-39; DOI: 10.21660/2026.144.5440

INFLUENCE OF NONLINEARITY ON THE LOAD BEARING CAPACITY OF STEEL STRUCTURES

*Aibek B. Yelubayev[1], Yerik T. Bessimbayev[2], Assel T. Ospanova[3] and Ulugbek T. Begaliyev[4]

[1,2,3]Institute of Architecture and Civil Engineering, Satbayev University; Kazakhstan
[4]International University of Innovative Technologies; Kyrgyzstan

*Corresponding Author, Received: 18 Jan. 2026, Revised: 25 Apr. 2026, Accepted: 07 May 2026

ABSTRACT: The nonlinear behavior of steel structures has a significant effect on both their safety and the efficiency of material usage. In real structures, the influence of physical nonlinearity associated with the onset and development of plastic deformations, as well as geometric nonlinearity due to second-order effects, cannot be ignored, especially for slender and spatial systems. This study examines the combined influence of material and geometric nonlinearity on the behavior of steel structures by comparative numerical analysis. The novelty of the study lies in the combined use of GOST (government standard) and EN-based stress–strain curves within a 3D LIRA-FEM 2024 model for direct comparison of linear and nonlinear structural response. A 3D industrial steel frame composed of columns, roof trusses, and vertical and horizontal bracing was investigated using both linear and nonlinear FEM (finite element method) formulations. The frame response was evaluated under representative ULS (ultimate limit state) and SLS (serviceable limit state) load combinations formed in accordance with EN 1990, using actions defined in EN 1991. Geometric nonlinearity was accounted for through a large-displacement formulation of nonlinear finite elements, without introducing explicit code-based initial geometric imperfections, while material nonlinearity was represented by nonlinear stress–strain behavior. The comparison showed that the nonlinear analysis generally led to higher displacements and a redistribution of internal forces relative to the linear model, with corresponding changes in stress patterns. The results indicate that accounting for nonlinear effects provides a more realistic assessment of structural performance and can support more rational steel consumption while maintaining structural reliability.

Keywords: Steel structures, Material Nonlinearity, Geometric Nonlinearity, Nonlinear Finite Element, Industrial Steel Frame, Second-Order Effects, LIRA-FEM

1. INTRODUCTION

The design and analysis of steel structures have traditionally been based on first-order theory (linear analysis), which assumes a linear relationship between loads and deformations and, consequently, a geometrically invariant structural configuration during loading. However, in real building operation, applied loads, local plastic deformations, initial geometric imperfections, and large displacements of members can significantly affect the stress–strain state and stability of the structure. In many cases, neglecting these factors leads to either a conservative overuse of steel or an underestimation of actual internal forces, ultimately reducing the structure's safety level.

Steel structures are widely used in industrial buildings, long-span roofs, multistorey frames, and energy-related facilities due to their high strength-to-weight ratio, rapid erection, and adaptability. These structures often operate under complex combinations of gravity, wind, crane, temperature, and seismic actions, where stability and second-order effects become critical. In practice, slender columns, flexible bracing systems, semi-rigid joints, and non-uniform load paths may amplify displacements and internal forces. Therefore, the realistic evaluation of structural response is essential not only for safety verification but also for rational material consumption and structural optimization. The relevance of nonlinear approaches further increases in performance-based design, retrofit, and strengthening tasks, and assessment of existing structures, where reserve strength, redistribution effects, and imperfection sensitivity must be adequately represented.[1–3]

Moreover, the increasing use of slender high-strength steel members, long-span roof systems, and modular industrial structures intensifies sensitivity to second-order effects and imperfections. This is particularly relevant for facilities with strict serviceability and stability requirements (e.g., process units, pipe-rack systems, and energy infrastructure), where small additional lateral drifts may substantially increase member forces and connection demands. Therefore, a clear engineering understanding of when linear assumptions remain acceptable and when nonlinear modeling becomes necessary is essential for both safe design and cost-effective detailing.[4,5]

The nonlinear behavior of steel and its influence on joint performance has been actively investigated for decades [6,7], and with the development of modern design standards—particularly EN 1993-1-1 and AISC-material and geometric nonlinearities have become essential elements of analytical models. EN 1993-1-1 permits both simplified linear methods using effective lengths [8,9] and more advanced second-order methods that directly account for material and geometric nonlinearity. Modern finite element software enables analysis in geometric and material nonlinear frameworks, expanding the potential for structural optimization and making the design process more reliable and closer to real behavior.

Recent studies on geometrically nonlinear analysis of steel frames have shown that the discrepancy between first-order and second-order results may become significant for systems with high slenderness, notable imperfections, and semi-rigid connections, especially under combined axial force, bending, and lateral loading. In such cases, nonlinear response may lead not only to increased displacements but also to a redistribution of internal forces between members and corresponding changes in joint demand, which affect both member utilization and the global stability margin. At the same time, despite the availability of advanced nonlinear tools in modern finite element software, linear approaches still dominate in routine engineering practice because of their simplicity, lower computational effort, and the lack of clear engineering guidance on when nonlinear modeling is necessary and how its results should be interpreted in design.

However, a practical research gap remains in providing a consistent engineering-oriented comparison of linear and nonlinear analyses for realistic steel building systems under identical loading scenarios, with emphasis on how internal forces and force redistribution evolve and how this affects the assessment of structural performance. The originality of this study lies in: (i) performing a direct comparative analysis of first-order (linear) and advanced nonlinear analysis for a representative steel building model; (ii) quantifying differences in key response parameters (e.g., axial forces, bending moments, displacement) and identifying the most sensitive members and zones; and (iii) demonstrating how nonlinear effects can change design demand and potential optimization decisions. The presented outcomes aim to support designers in understanding when nonlinear analysis is justified and how its results should be interpreted for safe and efficient steel design.

The remainder of this paper is organized as follows. Section 2 presents the research significance and summarizes the study's novelty and practical relevance. Section 3 describes the materials and methods, including the structural model, loading scenarios, and key assumptions for the linear and nonlinear analyses. Section 4 presents the calculation results and discussion, focusing on the analysis of internal forces, displacements, and force redistribution effects obtained from linear and nonlinear frameworks. Finally, the Conclusions section summarizes the main findings and implications for practical steel design, followed by the References.

2. RESEARCH SIGNIFICANCE

This study is significant because it clarifies how material and geometric nonlinearities influence the response of industrial steel frames and shows when simplified linear analysis may become insufficient. Its contribution lies in the consistent comparison of linear and nonlinear 3D analysis results for a steel frame model developed in LIRA-FEM 2024, with material behavior represented by stress–strain curves based on both GOST and EN provisions. The findings provide practical guidance for evaluating displacement growth, internal force redistribution, and the reliability of simplified design approaches. The results can support more rational assessment and design of steel structures, especially for slender members and joint-sensitive systems.

3. MATERIALS AND METHODS

3.1 Theoretical Background of Material Nonlinearity of Steel

Material nonlinearity in steel arises from the loss of proportionality between stress and strain as the applied load increases. At the initial stage of loading, the material exhibits elastic behavior governed by Hooke's law,

$$\sigma = E\varepsilon \qquad (1)$$

where σ is the normal stress, E is the modulus of elasticity (Young's modulus), and ε is the normal strain.

In this stage strains are directly proportional to stress. Upon reaching the yield point, plastic flow begins, accompanied by the accumulation of residual deformations and the redistribution of stress. Further increase in deformation leads to strain hardening and a gradual approach to the ultimate state, beyond which failure occurs. From the constitutive point of view, this behavior may be represented by an idealized stress–strain model including the elastic stage, yielding, strain hardening, and the limiting strain ε_u. Such idealization makes it possible to account for stiffness degradation and plastic redistribution in the nonlinear analysis of steel structures.

3.2 Classification of Steel According to GOST and EN

To illustrate the material nonlinearity of steel, stress–strain ($\sigma-\varepsilon$) diagrams were constructed for the main classes of structural steels specified in the GOST and EN standards. The diagrams reflect the characteristic stages of material behavior, including the elastic range up to the yield point, the yield plateau (typical of low-carbon steels according to GOST), the strain-hardening region (typical of EN steels and high-strength GOST steels), and the terminal stage corresponding to the limiting strain εu. The resulting stress–strain diagrams and the adopted mechanical parameters are presented in Figures 1 and 2 and Tables 1 and 2.

Material nonlinearity of steel is associated with the deviation from the linear elastic stress–strain relationship after the yield point is reached. In the elastic range, the material response follows Hooke's law, while after yielding the behavior depends on the adopted constitutive model and may include a yield plateau, strain hardening, and a terminal limiting strain. For low-carbon steels, the nonlinear response is typically characterized by a pronounced yield plateau and a higher plastic reserve, whereas higher-strength steels generally exhibit a shorter plastic range and reduced ductility. In the present study, these features were represented by user-defined stress–strain diagrams in LIRA-FEM, based on the adopted values of elastic modulus, yield strength, ultimate strength, and limiting strain for each steel grade. Such an idealization makes it possible to account for stiffness degradation and plastic redistribution of internal forces in the nonlinear analysis of steel structures.

In the calculations, structural steel grades according to GOST 27772–2021 [10](C245, C255, C345, C355, C390, and C440) were used, for which the elastic modulus was taken as E = 206000 MPa. The minimum failure strain at fracture ranges from 0.15-0.20 for low-carbon steels C245 and C255 to 0.12 for high-strength steel C440. For steel specified in EN 10025-2, represented by grades S235, S275, S355, and S450 [11], the elastic modulus was taken as E =210000 MPa, while the failure strain ranges from 0.12 to 0.20 for the high-strength grade S450 [12].

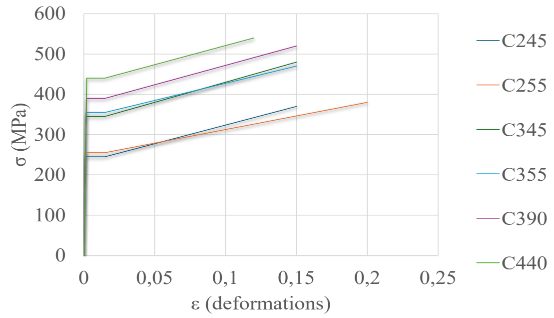

Fig.1 Stress–strain (σ–ε) diagram for structural steels according to GOST 27772–2021 [10].

Table 1. Mechanical properties and constitutive parameters of GOST 27772-2021 [10] steels adopted for nonlinear analysis

Steel grade	E, MPa	fy, MPa	fu, MPa	εu
C245	206000	245	370	0,15
C255	206000	255	380	0,20
C345	206000	345	490	0,12
C355	206000	355	470	0,15
C390	206000	390	520	0,15
C440	206000	440	540	0,12

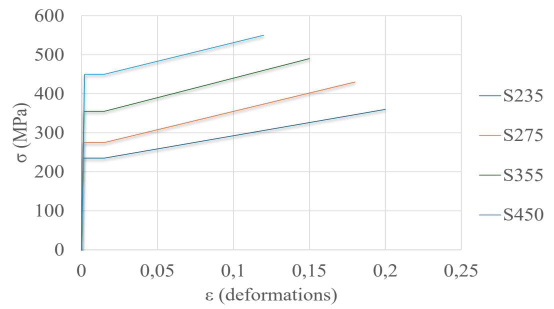

Fig.2 Stress–strain (σ–ε) diagram for structural steels according to EN 10025–2 [11].

Table 2. Mechanical properties and constitutive parameters of EN 10025–2 [11] steels adopted for nonlinear analysis

Steel grade	E, MPa	fy, MPa	fu, MPa	εu
S235	210000	235	360	0,2
S275	210000	275	430	0,18
S355	210000	355	490	0,15
S450	210000	440	550	0,12

Steels according to EN 10025-2 display a smoother transition from the elastic to the plastic stage and almost no pronounced yield plateau. Analysis of the σ–ε diagrams shows that low-carbon steels of domestic standards exhibit a distinct yield plateau and a significant plastic reserve, whereas EN steels exhibit a more smoothly bilinear behavior. High-strength steels in both standard systems exhibit lower elongation at fracture, as shown in the diagrams (Figures 1 and 2). The constructed σ–ε curves, based on normative values for yield strength, ultimate strength, and limiting strain, were subsequently used to account for material nonlinearity in load-bearing capacity calculations of steel structures. In LIRA-FEM, the default elastic material representation was supplemented by user-defined multilinear stress–strain diagrams, which made it possible to describe the elastoplastic behavior of the adopted steel grades in the nonlinear analysis. The limiting strain εu was taken as the terminal point of the adopted constitutive diagram.

3.3 Geometric Nonlinearity

Geometric nonlinearity arises from the modification of the structural stress–strain state caused by large displacements and rotations of structural members. Such deformations may alter system's spatial configuration, which in turn affects its overall stiffness and internal force distribution. In contrast to linear first-order analysis, in which the structural configuration is assumed to remain unchanged during loading, geometric nonlinear analysis enables consideration of the force redistribution resulting from changes in geometry throughout the loading process [13].

From the analytical standpoint, two principal approaches are adopted:

• First-order (linear) analysis - assumes that deformations are sufficiently small and the structural configuration remains unchanged under applied loads; internal forces are determined exclusively by external loading.

• Second-order (geometrically nonlinear) analysis - accounts for changes in the structural configuration during loading and the accompanying additional second-order internal forces.

The manifestations of geometric nonlinearity are conventionally represented through the P–Δ and P–δ effects:

• P-Δ effect (global second-order effect) considers the influence of the overall lateral displacements of the structural system on the axial load effects. When significant lateral displacements occur, the vertical compressive load P induces additional bending moments, which may cumulatively lead to overall frame instability or global buckling (see Fig. 3).

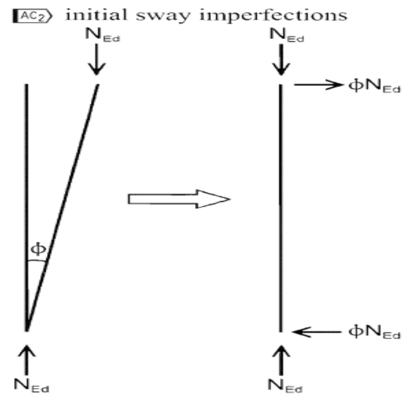

Fig.3 Global imperfections [14]

P–δ effect (local second-order effect) reflects the influence of the curvature of individual members and the increase of bending moments within the members under axial compression. According to [15], the P–δ effect may significantly influence the axial force, especially in thin-walled sections. Therefore, in the proposed plastic hinge method, the bowing effect is obligatorily considered in the axial strain formulation, thereby minimizing errors in force prediction.

Thus, the general expression for second-order bending moments can be written as Eq.2.

$$M_{II} = M_I + P \times \Delta + P \times \delta \quad (2)$$

where M_I is the first-order bending moment, $P \times \Delta$ is the bending moment due to global imperfections, and $P \times \delta$ is the bending moment due to local imperfections

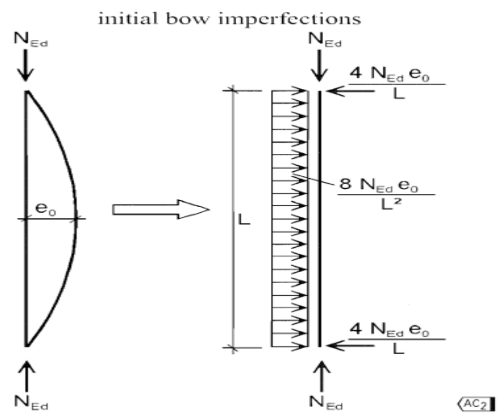

Fig.4 Local imperfections [14]

In practical structural analysis, several methods are used to introduce global imperfections (EN 1993-1-1) [14].

Eigenmode imperfection method – geometric imperfections are introduced into the analytical model based on the first (or a combination of several) buckling mode shapes obtained from a linear eigenvalue buckling analysis.

Notional load method – equivalent horizontal forces are applied to simulate initial sway imperfections of the frame. The notional load factor is calculated using Eq. 3 [14].

$$\varphi = \varphi_0 \alpha_h \alpha_m \quad (3)$$

where $\varphi_0 = 1/200$ is the basic imperfection amplitude, $\alpha_h = 2/3 \leq \alpha_h \leq 1.0$ is the coefficient dependent on the column height, and $\alpha_m = \sqrt{0.5(1 + 1/m)}$ is the coefficient dependent on the number of columns in the row.

Direct modelling method — imperfections are introduced by explicitly displacing the nodes of the analytical model. This approach is labor-intensive for large structural systems but allows arbitrary imperfection shapes to be defined.

For local imperfections, EN 1993-1-1 (Table 4.1) [14] specifies the initial out-of-straightness amplitude in the form of the ratio e_0/L, which depends on the buckling curve classification.

Table 3. Design values of initial local bow imperfections [14]

Buckling curve	e_0/L (elastic analysis)	e_0/L (plastic analysis)
a_0	1/350	1/300
a	1/300	1/250
b	1/250	1/200
c	1/200	1/150
d	1/150	1/100

In AISC 360-22, a constant value of $L/1000$ is adopted. If this limit is exceeded, a full second-order analysis is performed, or the member stiffness is reduced by applying an effective flexural rigidity $(EI)_{\text{eff}} = 0.8EI$, and fictitious horizontal loads are introduced (typically 0.2% of the vertical loads). This approach enables a partial consideration of both geometric and material nonlinearity without performing a full advanced second-order analysis [16].

3.4 Influence of geometric nonlinearity on joints

The stiffness of joints in framed structures significantly influences on the manifestation of P–Δ effects and the redistribution of internal forces within the system and has been investigated for an extended period. Incorrect idealization of boundary conditions (e.g., modelling joints as fully pinned or fully rigid) may lead to distortion of the internal force distribution, particularly bending moments, which ultimately affect the load-carrying capacity of the joints and adjacent members. A number of studies, including [17], have demonstrated that accounting for semi-rigid joint behavior has a substantial effect on the distribution of actions and displacements within the frame, and that the use of appropriate modelling techniques, such as those introduced in [18] allows for correct representation of the moment–rotation behavior of joints and prevents underestimation of deformations.

In advanced numerical approaches, such as the refined plastic hinge model proposed in [19], residual plastic deformations in the joint region are also considered. This enables a more realistic description of the behavior of semi-rigid joints under combined geometric and material nonlinearity, particularly when the rotational stiffness exhibits a stochastic nature.

The classification criterion for joints in EN 1993-1-8 [20] is the initial rotational stiffness $S_{j,ini}$, which is compared against expressions involving the ratio EI/L of the corresponding frame members. Semi-rigid joints possess finite stiffness, and for their correct representation a bilinear moment rotation relationship is recommended, reflecting connection plasticity and the gradual decrease of rotational stiffness with increasing rotation demand (Figure 5). In addition, study [15] proposes a model employing finite-stiffness rotational springs, differentiated for the major and minor axes of the section (Figure 6). Such modelling refinement enables more accurate representation of the elasto-plastic behavior of joints, particularly for H-shaped sections, where the moment–rotation response in-plane and out-of-plane differs substantially.

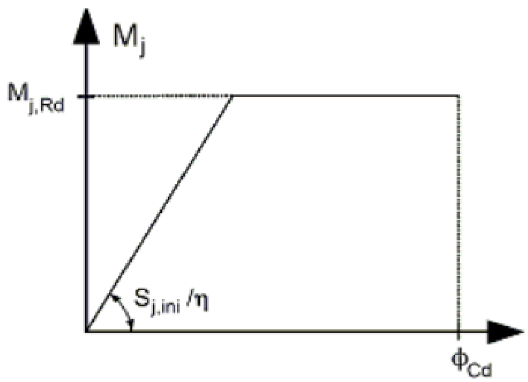

Fig.5 Simplified bilinear moment–rotation relationship for a semi-rigid joint [20]

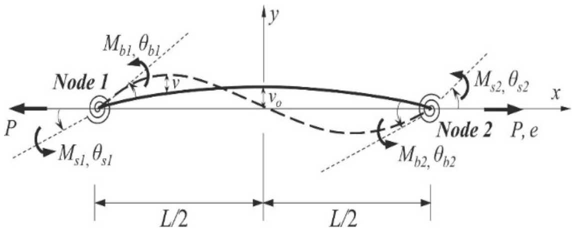

Fig.6 Beam–column element model with plastic hinges [15]

Modelling of semi-rigid joints within the structural analytical model may be performed using the following approaches:

• By means of rotational spring elements, representing the rotational stiffness of the joint, as demonstrated in [15];

• Through the effective stiffness approach, in which the rotational stiffness is averaged and incorporated into the member stiffness formulation;

• By direct joint modelling, where all joint components (plates, angles, bolts, etc.) are explicitly represented in the analytical model, which increases modelling accuracy but significantly raises computational effort.

Consideration of actual joint stiffness is particularly important in flexible structural systems, since increasing rotational deformations intensify P–Δ effects and may lead to premature global instability.

As demonstrated in [13], the stiffness of joints and supports has a significant influence on the manifestation of P–Δ effects. Incorrect assessment of rotational boundary conditions in the effective buckling length method may lead to inaccurate estimation of internal force effects in frame members and, consequently, to improper design of joint components. According to EN 1993-1-8 [20] (Figure 7 and Table 4), structural joints are classified as follows:

Table 4. Joint types and classification criteria

NO.	Joint type	Classification criterion
1	Rigid joint	$S_{j,\,ini} \geq 25EI_b/L_{j,\,b}$
2	Semi-rigid joint	$0.5EI_b/L_{j,\,b} \leq S_{j,\,ini} \leq 25EI_b/L_{jb}$
3	Nominally pinned joint	$S_{j,\,ini} = 0.5EI_b/L_{jb}$

where $S_{j,\,ini}$ is the initial rotational stiffness of the joint, EI_b is the flexural stiffness of the beam, and L_b is the beam span.

4. CALCULATION AND RESULTS

This section presents an analysis of a steel frame structure using first-order and second-order theories. For this purpose, the standard iterative Newton–Raphson procedure [21–23] was used due to its computational efficiency. The investigated structural system is a three-dimensional frame consisting of columns, trusses, bracing members, and purlins, modelled in the LIRA-FEM software package with the capability of performing second-order analysis.

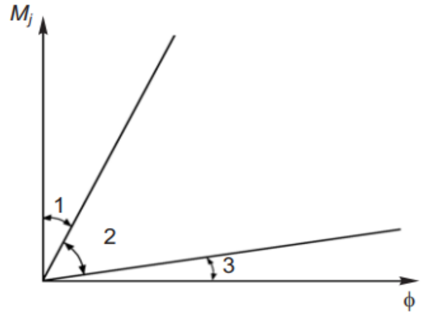

Fig.7 Joint classification by rotational stiffness [20]

The primary objective is to evaluate the influence of geometric nonlinearity (P–Δ effects) on displacements, internal forces, load-carrying capacity, and steel consumption in both members and joints. The analytical model represents an idealized steel frame with 18 m spans, 6 m column spacing, and a total height of 11.9 m. The main structural components include:

•Vertical steel columns (steel grade C255); [10]

•Trusses (steel grade C245); [10]

•Vertical and horizontal bracing members (steel grade C245); [10]

• Secondary members - purlins (steel grade C245); [10]

The applied actions include self-weight, permanent and variable imposed loads, as well as snow and wind actions according to EN 1991. The adopted rolled steel sections and the corresponding member groups are summarized in Table 5.

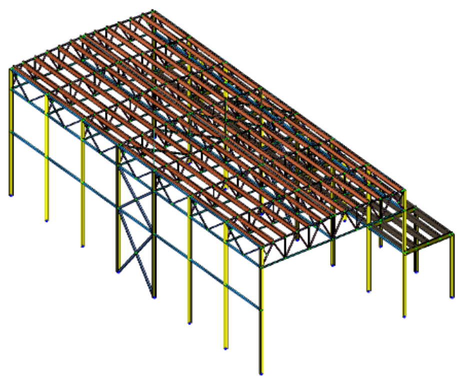

Fig.8 3D view of steel frame system (frames and bracing)

Table 5 Cross-sectional properties of elements

Member group	Section designation	A, cm²	Iy, cm⁴	Iz, cm⁴
Columns	30K1	108.0	18110	6079.0
Purlins	20U	23.40	1520	113.0
Roof truss top chord	L100x100x10	19.24	178.95	178.95
Roof truss bottom chord	L100x100x8	15.6	147.19	147.19
Truss diagonals	L100x100x8	15.6	147.19	147.19
Vertical bracing	180x5.5	37.61	1888	1888
Horizontal bracing	100x5	18.36	270.9	270.9

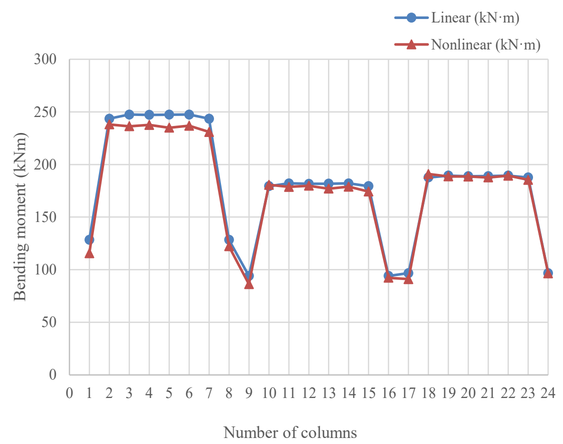

Fig.9 Bending moment (M_y) diagram for linear and nonlinear analysis

4.1 Results discussion

The presented results demonstrate that the consideration of geometric nonlinearity leads to an increase in horizontal displacements and to changes in the distribution of axial forces and bending moments in individual columns by 2.36% and 2.23%, respectively (Table 6). The member-wise redistribution of axial forces and horizontal displacements is shown in Figures 9,10 and 11 where the column numbering along the horizontal axis makes it possible to identify the locations of the largest deviations between the linear and nonlinear analyses. In particular:

• The maximum horizontal displacement under load combination No. 43 according to Equation (6.14b) increased from 19.4 mm to 38.1 mm, corresponding to a growth of +96.4%, with the serviceability limit taken as L/250

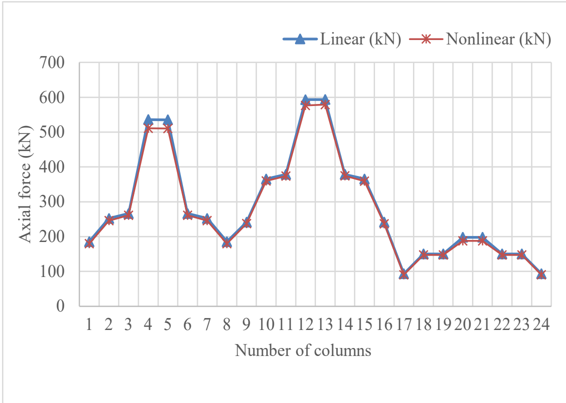

Fig.10 Axial force (N) diagram for linear and nonlinear analysis

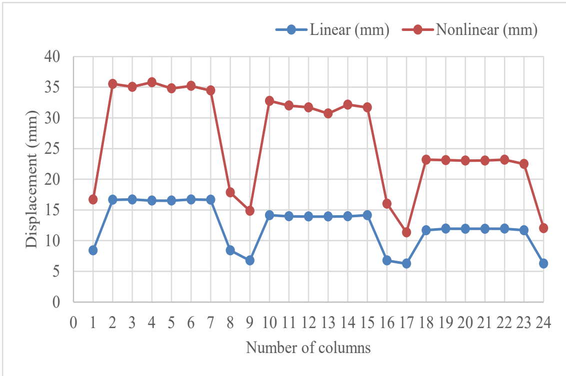

Fig.11 Displacement (mm) diagram along X-axis for linear and nonlinear analysis

• The maximum axial force in the columns under the most unfavorable load combination decreased from 593 kN to 579 kN (−2.36%);

• The maximum bending moment My in the columns decreased from 243.511 kNm to 238.083 kNm (−2.23%).

The reduction in internal force demand when considering geometric nonlinearity is associated with changes in the stiffness distribution within the structure. In the nonlinear analysis, the stiffness of the columns was reduced, resulting in a higher proportion of horizontal load resistance provided by the bracing members. Consequently, during section optimization, the dimensions of both horizontal and vertical bracing members were increased, leading to a more favorable redistribution of internal forces and, therefore, a decrease in bending moments and axial forces in the columns.

Furthermore, it was established that the inclusion of P–Δ effects enables optimization of the total steel mass of the structure. The resizing of bracing members was performed automatically in the LIRA-FEM environment on the basis of the adopted design checks, including strength and stability requirements. The final selected sections satisfied the corresponding code-based criteria used in the calculation model. The total weight of the steel frame obtained from linear analysis was 1174.06 kN, whereas the model incorporating geometric nonlinearity resulted in 1083.00 kN, corresponding to a reduction of 7.756%.

At the steel detailing stage, where the total steel quantity is traditionally increased by 4% to account for connection plates, stiffeners, gussets, bolts, welds and other fabrication and assembly components, this allowance was adopted on the basis of common engineering practice, according to which the additional steel consumption at the detailing stage usually does not exceed 4%. The final weights were:

- 1126.32 kN — nonlinear analysis;
- 1221.02 kN — linear analysis;

Thus, the resulting reduction in steel consumption at the steel detailing stage remains 7.756%, confirming the feasibility and effectiveness of second-order analysis for cross-section optimization and for reducing steel tonnage.

Table 6. Structural behavior analysis.

NO.	Parameters of internal force diagrams	Linear analysis	Nonlinear analysis	Changes, %
1	Maximum horizontal displacements under SLS (mm)	19.4	38.1	+96.4
2	Maximum axial forces in columns under ULS (kN)	593.449	578.721	-2.36
3	Maximum bending moment My in columns (kNm) under ULS	243.511	238.083	-2.23
4	Total weight of the steel frame including detailing stage (kN)	1221.02	1126.32	-7.756

5. DISCUSSION

1. The consideration of geometric nonlinearity in the analysis of a steel frame leads to a significant change in the structural stress–strain response. The maximum horizontal displacements increased from 19.4 mm to 38.1 mm (+96.4%). At the same time, a slight reduction in axial forces (−2.36%) and bending moments (−2.23%) in the columns is observed due to stiffness redistribution.

2. A reduction in column stiffness in the nonlinear analysis increased the contribution of horizontal and vertical bracing members. Enlarging the bracing cross-sections provided internal force redistribution and partially reduced axial forces and bending moments in the main load-bearing elements.

3. Semi-rigid joints together with bracing systems intensify second-order (P–Δ) effects, influencing structural behavior and causing internal force redistribution. Neglecting these effects may lead to underestimation of displacements and reduced computational accuracy.

4. Differences between linear and geometrically nonlinear analysis are especially significant for flexible frame systems sensitive to deformations.

5. Considering geometric nonlinearity and P–Δ effects improves analytical accuracy and contributes to steel consumption optimization. The total steel mass obtained from nonlinear analysis amounted to 1083 kN, compared to 1174.06 kN from linear analysis (−7.76%). At the steel detailing stage, with a 4% addition for connection components, the reduction remained at 7.756%.

6. The results are consistent with international research [15,19,24,25] and confirm the feasibility of second-order analysis at the design stage.

6. CONCLUSION

This study demonstrated the significant influence of both material and geometric nonlinearities on the behavior of steel frame structures. To account for material nonlinearity, stress–strain (σ–ε) diagrams were developed for steels according to GOST 27772–2021 and EN 10025-2, based on the normative values of yield strength, ultimate tensile strength, and limiting strain. The analysis showed that low-carbon steel according to GOST exhibits a pronounced yield plateau and a considerable plastic reserve, whereas EN steels demonstrate a smoother elastoplastic transition. High-strength steels in both classification systems possess reduced ductility, which must be taken into consideration in elastoplastic analysis. The developed curves were used to model material behavior within the plastic deformation range using user-defined diagrams in LIRA-FEM.

Geometric nonlinearity, considered through second-order effects associated with large displacements, had a noticeable influence on the redistribution of internal forces, displacements, and the overall stability of the frame. Numerical modelling results showed that:

- the maximum horizontal displacements increased by 96.4%;

• the maximum axial forces in columns decreased by 2.36%;

• the maximum bending moments in columns decreased by 2.23%;

• the total steel mass decreased by 7.76% compared with linear analysis, indicating the potential for cross-sectional optimization when accurate second-order modelling is applied.

The findings demonstrate that neglecting material and geometric nonlinearities may lead to a non-conservative assessment of structural response, especially with respect to lateral displacements and internal force redistribution. At the same time, the conclusions of the present study should be interpreted within the limitations of a single case study based on one three-dimensional industrial steel frame. In addition, the study did not include nonlinear dynamic or seismic analysis, and the obtained results are therefore limited to the considered static loading scenarios.

From a practical design viewpoint, the applicability of simplified first-order analysis should be verified in accordance with Clause 5.2 of EN 1993-1-1. Where the Eurocode criterion is not satisfied, second-order effects should be considered explicitly.

Overall, the conducted research confirms that the combined consideration of material and geometric nonlinearities provides a more reliable prediction of the structural stress–strain response and may improve the economic efficiency of engineering design solutions for steel frame systems.

7. REFERENCES

1. Ziemian C.W., Ziemian R.D., Efficient geometric nonlinear elastic analysis for design of steel structures: Benchmark studies. Journal Constructional Steel Research, Vol.186, 2021, 106870. https://doi.org/10.1016/j.jcsr.2021.106870
2. Nguyen T. D., Vu Q.A., Analysis of steel frame with semi-rigid connections and constraints using a condensed finite element formulation. International Journal of GEOMATE, 25(111), 2023, pp. 113-121. https://doi.org/10.21660/2023.111.4022
3. Quan C., Kucukler M., Gardner L., Out-of-plane stability design of steel beams by second-order inelastic analysis with strain limits, Thin-Walled Structures, Vol.169, 2021, 108352. https://doi.org/10.1016/j.tws.2021.108352
4. Jiwapatria S., Setio H.D., Sidi I.D., Kusumaningrum P., Performance level improvement of steel frame building equipped with optimized active tendon system. International Journal of GEOMATE, 27(123), 2024, pp. 1–10. https://doi.org/10.21660/2024.123.4575
5. Bai R., Liu S.-W., Liu Y.-P., Chan S.-L., Direct analysis of tapered-I-section columns by one-element-per-member models with the appropriate geometric-imperfections. Engineering Structures, Vol.183, 2019, pp. 907–921. https://doi.org/10.1016/j.engstruct.2019.01.021
6. Nguyen Q.-B., Nguyen H.-H., Ha M.-H., An efficient framework for optimization of nonlinear steel trusses with continuous variables using LightGBM. International Journal of GEOMATE, 26(116), 2024, pp. 85-92. https://doi.org/10.21660/2024.116.4398
7. Walport F., Gardner L., Real E., Arrayago I., Nethercot D.A., Effects of material nonlinearity on the global analysis and stability of stainless steel frames. Journal of Constructional Steel Research, Vol.152, 2019, pp. 173–182. https://doi.org/10.1016/j.jcsr.2018.04.019
8. Mu Z., Xu Y., Yang Y., Fan Z., Study of Effective Length Factor of Frame–Core Wall Structure with Cross-Layer Columns. Applied Sciences, 13(12), 2023, 6875. https://doi.org/10.3390/app13126875
9. Li G.-Q., Cao K., Lu Y., Column effective lengths in sway-permitted modular steel-frame buildings. Proceedings of the Institution of Civil Engineers-Structures and Buildings, 172(1), 2019, pp. 30-41. https://doi.org/10.1680/jstbu.17.00006
10. GOST 27772–2021, Rolled Products for Structural Steel Constructions, General Specifications, 2021.
11. EN 10025-2, Hot rolled products of structural steels – Part 2: Technical delivery conditions for non-alloy structural steels, 2019.
12. Eurocode 3: Design of steel structures - Part 1-5: Plated structural elements, 2006.
13. Zhang Z.-J., Chen B.-S., Bai R., Liu Y.-P., Non-linear behavior and design of steel structures: Review and outlook. Buildings, 13(8), 2023, 2111. https://doi.org/10.3390/buildings13082111.
14. Eurocode 3: Design of steel structures - Part 1-1: General rules and rules for buildings, 2005.
15. Tang Y-Q, Zhu H, Liu Y-P, Ding Y-Y, Chan S-L. A novel efficient plastic hinge approach for direct analysis of steel structures. Engineering Structures, Vol.319, 2024, 118837.

https://doi.org/10.1016/j.engstruct.2024.118837

16. ANSI/AISC 360-22, Specification for Structural Steel Buildings, American Institute of Steel Construction, 2022.
17. Balaban Y., Fırat Alemdar Z., Alemdar F., Nonlinear Inelastic Analysis of Semi-Rigid Steel Frames with Top-and-Seat Angle Connections. Buildings, 16(2), 2026, pp. 408. https://doi.org/10.3390/buildings16020408
18. Lemes Í.J.M., Silveira R.A.M., Teles L.O.M., Barros R.C., Silva A.R.D., Numerical formulation for advanced non-linear static analysis of semi-rigid planar steel frames. Journal of the Brazilian Society of Mechanical Sciences and Engineering, Vol.45, 2023, 358. https://doi.org/10.1007/s40430-023-04288-6
19. Dang H.-K., Thai D.-K., Kim S.-E., Stochastic analysis of semi-rigid steel frames using a refined plastic-hinge model and Latin hypercube sampling. Engineering Structures, Vol. 291, 2023. https://doi.org/10.1016/j.engstruct.2023.116313
20. Eurocode 3: Design of steel structures–Part 1-8: Design of joints, 2005.
21. Sun B., Zeng Z., Zhang Y., Shen W., Ou J., An effective geometric nonlinear analysis approach of framed structures with local material nonlinearities based on the reduced-order Newton-Raphson method. Soil Dynamics and Earthquake Engineering, Vol.172, 2023, 107991. https://doi.org/10.1016/j.soildyn.2023.107991
22. Farman M., Akgül A., Alshaikh N., Azeem M., Asad J., Fractional-order Newton–Raphson method for nonlinear equation with convergence and stability analyses. Fractals, Vol.31, No.10, 2023, 2340079 https://doi.org/10.1142/S0218348X23400790
23. Sun B., Zhang Y., Dai D., Wang L., Ou J., Seismic fragility analysis of a large-scale frame structure with local nonlinearities using an efficient reduced-order Newton-Raphson method. Soil Dynamics and Earthquake Engineering, Vol. 164, 2023, 107559 https://doi.org/10.1016/j.soildyn.2022.107559
24. Iu C. K., Bradford M., Higher-order non-linear analysis of steel structures: Part I: elastic second-order formulation. Advanced Steel Construction, 8(2), 2012, pp. 168-182.
25. Frye M.J., Morris G.A., Analysis of flexibly connected steel frames. Canadian Journal of Civil Engineering, Vol. 2, No. 3, 1975. https://doi.org/10.1139/l75-026.